INTERNATIONAL JOURNAL OF OPTIMIZATION IN CIVIL ENGINEERING
Int. J. Optim. Civil Eng., 2022; 12(1):105-123

LARGE-SCALE DOME TRUSS OPTIMIZATION WITH FREQUENCY CONSTRAINTS USING EVPS ALGORITHM

A. Kaveh[1], P. Hosseini[2*, †], N. Hatami[3] and S. R. Hoseini Vaez[3]
[1]*School of Civil Engineering, Iran University of Science and Technology, Tehran, Iran*
[2]*Faculty of Engineering, Mahallat Institute of Higher Education, Mahallat, Iran*
[3]*Department of Civil Engineering, Faculty of Engineering, University of Qom, Qom, Iran*

ABSTRACT

In recent years many researchers prefer to use metaheuristic algorithms to reach the optimum design of structures. In this study, an Enhanced Vibrating Particle System (EVPS) is applied to get the minimum weight of large-scale dome trusses under frequency constraints. Vibration frequencies are important parameters, which can be used to control the responses of a structure that is subjected to dynamic excitation. The truss structures were analyzed by finite element method and optimization processes were implemented by the computer program coded in MATLAB. The effectiveness and efficiency of the Enhanced Vibrating Particle System (EVPS) is investigated in three large-scale dome trusses 600-, 1180-, and 1410-bar to obtain the weight optimization with frequency constraints.

Keywords: optimization; dome truss structures; frequency constraints; metaheuristic algorithms; Enhanced Vibrating Particle System.

Received: 20 November 2021 Accepted: 22 January 2022

1. INTRODUCTION

Although structural weight optimization has frequently been investigated by many researchers, and its history goes back many decades, it is still one of the most challenging and desired problems to be studied. Since the dynamic behavior of structures largely depends on their modal characteristics, frequency constraints play a significant role in assessing and safe design of structures. When the frequency constraints are taken into account in the design process, structural optimization becomes a nonlinear and non-convex problem. In vibration problems with low-frequency, the response of the structure primarily

[*]Corresponding author: Faculty of Engineering, Mahallat Institute of Higher Education, Mahallat, Iran
[†]E-mail address: P.Hosseini@mahallat.ac.ir (P. Hosseini)

depends on its fundamental frequencies and mode shapes (Grandhi, 1993) [1]. The dynamic behavior of the structure can therefore be restricted by these parameters. The objective of optimization for a frequency constraint problem is to minimize the weight of the structure for which some natural frequencies are limited in the upper bound and/or lower bound.

Structural optimization with frequency constraints has been considered remarkably in the last decades. Optimization problems aren't able to be solved with the popular mathematical methods due to their limitations, such as requiring gradient data, sensitivity to the starting point, and enormous computational calculations. On the other hand, using classical optimization methods is not applicable because they may be trapped in local optimum which causes undesired design solutions. By increasing the number of variables, the problem becomes more complicated and multiple structural analyses are required to implement the structural optimization. In a frequency constraint optimization problem, the structural analyses involve large generalized eigenproblems to find the natural frequencies. The dimensions of the involved matrices and the required computational time and effort increase with the size of the structure are optimized. Thus, integrating impressive eigensolution methods which help reduce the computational time of a single structural analysis could be very useful, especially when large structures are optimized. To solve the above-mentioned problems and weaknesses, researchers invented metaheuristic algorithms that are less time-consuming and obtain better solutions. Several metaheuristic algorithms recently have been used to get an optimal design of structures. Das and Saha (2021) used various kinds of metaheuristic algorithms such as Eagle Perching Optimization, Dragonfly Algorithm, Bird Swarm Algorithm, Whale Optimization Algorithm, Firefly Algorithm Flower Pollination Algorithm to observe real-life structural safety [2]. Houssein et al. (2021) proposed new metaheuristic algorithms called Lévy flight distribution (LFD) to solve real optimization problems [3]. Ficarella et al. (2021) investigated the advanced form of three metaheuristic algorithms of Big Bang-Big Crunch (BBBC), Simulated Annealing (SA), Harmony Search (HS) to minimize the weight of four skeletal structures [4].

The optimization under frequency limitations using metaheuristic algorithms has been investigated by many researchers. Kaveh and Zolghadr (2014) offered a new algorithm named Democratic Particle Swarm Optimization (DPSO) to solve optimization problems with frequency constraints [5]. Kaveh and Mahdavi (2014) introduced a new method to solve optimization under frequency restriction named Colliding-Bodies Optimization (CBO) [6]. An Enhanced Colliding-Bodies Optimization (ECBO) which is the upgrade version of CBO, was suggested by Kaveh and Ghazan (2014) to design optimal structures [7]. Kaveh et al. (2015) suggested the Dolphin Echolocation (DE) algorithm for optimum design of structure under dynamic limitations [8]. Jalili and Hosseinzade (2018) proposed a new integrated migration and differential evolution strategies (MS–DE) algorithm to perform optimization of truss structures with multiple dynamic constraints [9].

A dome truss structure is essentially a triangulated system of straight interconnected structural elements. The most common use of trusses is stadiums, skylight roofs, exhibition halls, greenhouses stadiums, skylight roofs, exhibition halls, greenhouses. Covering large spans, no need for internal columns, lightweight, easy production, compatibility with the environment, and architectural beauty are the main reasons for using trusses. Therefore, many optimization types of research have been done about dome truss structures. Kaveh et

al. (2021) used the Quantum-based Jellyfish Search (QJS) algorithm which is the developed version of Jellyfish Search (JS) to solve structural optimization problems. These algorithms are inspired by the food-finding behavior of jellyfish in the ocean [10]. Carlos et al. (2020) proposed a new modified version of the social engineering optimizer (SEO), called MSEO, for size and shape optimization of truss structures considering frequency constraints [11]. Jalili et al. (2019) introduced the Cultural Algorithm (CA) to solve optimization. This algorithm is inspired by the principles of human social evolution. The overall framework of CA is modeled based on the biocultural evolution, in which genes and culture are two interacting forms of inheritance [12]. Grzywiński et al. (2020) designed the plane and spatial truss structures by a popular metaheuristic optimization technique termed Teaching Learning-Based Optimization (TLBO) [13]. Carlos et al. (2019) used the Modified Simulated Annealing Algorithm (MSAA) for size and shape optimization of truss structures with frequency constraints [14]. Jalili et al. (2017) proposed the Charged System Search (CSS) algorithm with Migration-based Local Search (MBLS) for resolving optimization problems with frequency constraints [15]. Kaveh et al. (2021) introduced an Enhanced Forensic-Based Investigation (EFBI) for the optimal design of frequency-constrained dome-like trusses. The Forensic-Based Investigation (FBI) algorithm is inspired by the criminal investigation process [16]. Tejani et al. (2017) suggested an improved version of Symbiotic Organisms Search (SOS) named an Improved SOS (ISOS) to conquer the problems of optimal design [17]. Makiabadi et al. (2021) applied the Enhanced Symbiotic Organisms Search (ESOS) algorithm for design optimization of trusses with frequency constraints [18]. Lemonge et al. (2021) adopted a modified version of the Differential Evolution termed the Third Evolution Step Differential Evolution (GDE3) for optimization truss structures considering natural frequencies [19].

Also many studies have been done to investigate the optimization of large-scale dome truss with dynamic limitations. Lio et al. (2019) proposed a memory-based search strategy for the fruit fly optimization algorithm (FOA) to enrich its searchability and utilize an improved Deb (IDeb) rule to tackle the constraints and increase the computational efficiency of the FOAs [20]. Kaveh and Zolghadr (2017) applied a Cyclical Parthenogenesis (CP) algorithm to reach optimization under frequency constraints [21]. Shahrouzi et al. (2018) proposed a method called teaching–learning-based optimization and bat-algorithm to design large truss as optimum as necessary [22]. Kaveh et al. (2021) introduced the Water Strider Algorithm (WSA) algorithm which diversifies the solutions and focuses on promising areas during the iterations [23]. Kaveh et al. (2019) applied Logistic map (CLFA) and Gaussian map (CGFA) algorithms to minimize the weight of large trusses under frequency constraints [24]. Other hybrid metaheuristc algorithm can be found in the work of Kaveh and MalakoutiRad [25]and Kaveh and Talatahri [26].

The Enhanced vibrating particle system (EVPS) is one of the metaheuristic algorithms that were recently proposed by some researchers to solve optimization problems. This algorithm is an improved version of vibrating particle systems (VPS), and the optimization results of this algorithm confirmed its performance. Kaveh and Ilchi Ghazaan (2017) introduced a new algorithm called vibrating particle systems (VPS), using viscous damping for free vibration of a single degree of freedom system [27]. Kaveh and Khosravian (2021) proposed vibrating particle systems (VPS) as an approach to solving optimization problems

[28]. Kaveh and Hoseini Vaez (2018) studied about two different trusses to show the performance of vibrating particle systems (VPS) and Enhanced vibrating particle systems (EVPS) algorithms in weight optimization of truss structures [29]. To demonstrate the performance of (VPS) and (EVPS) algorithms, Kaveh and Hoseini Vaez (2019) used different types of trusses, and they considered natural frequencies and mode shapes as the objective function. They realized that the answers resulting from EVPS are better than VPS [30]. Kaveh and Hoseini Vaez (2019) used Modified Dolphin Monitoring (MDM) operator to show the performance of EVPS and other metaheuristic algorithms [31]. Kaveh et al (2020) used EVPS to reach optimal design of the buckling restrained braced frames [32]. To calculate reliability index of four power transmission line towers, Hosseini et al. (2020) applied EVPS algorithm [33]. Kaveh et al. (2021) used modified dolphin monitoring to investigate the efficiency of EVPS algorithm to detect cracks in plate structures [34]. To design steel frame structures with reliability index, Kaveh et al (2021) applied VPS and EVPS algorithms [35].

In this study, the Enhanced vibrating particle system (EVPS) is used to reach the minimum weight of three large-scale dome trusses with frequency constraints, and the results are compared with DPSO [36], CBO and ECBO [37], and VPS [38] algorithms.

2. FORMULATION OF OPTIMIZATION

Layout optimization of truss structures with frequency constraints with sizing variables can be stated mathematically as:

$$\begin{gathered} Find\ X = [x_1.x_2 \ldots . x_n] \\ to\ minimize\ P(X) = f(X) \times f_{\text{penalty}}(X) \\ Subject\ to \\ \omega_j \le \omega_j^* for\ some\ natural\ frequnceis\ j \\ \omega_k \le \omega_k^* for\ some\ natural\ frequnceis\ j \\ x_{imin} \le x_i \le x_{imax} \end{gathered} \tag{1}$$

where *X* is the input vector with the cross-sectional areas of the members; *n* is the total number of input variables, which is selected with respect to element grouping; *f (X)* is the cost function, which can be taken as structural weight depending on the type of the problem; $f_{penalty}(X)$ is the penalty function, which magnifies the weight of the infeasible solutions in order to make the problem unconstrained. *P(X)* is the penalized cost function; ω_j and ω_j^* are the *j*th vibration frequency of the structure and its corresponding upper limit, respectively; ω_k and ω_k^* are the *k*th vibration frequency of the structure and its corresponding upper limit, respectively; x_{imin} and x_{imax} define the permissible range for the design variable x_i.

The weight of the structure as the cost function can be stated as:

$$f\ (X) = \sum_{i=1}^{nm} \rho_i L_i A_i \tag{2}$$

in which *nm* is the total number of structural members, ρ_i, *is* the material density, L_i, and A_i are the length, and cross-sectional area of the *i*th member, respectively.

In this study, a penalty function is used to make the optimization problem unconstrained. The idea is to magnify the weight of the candidate solutions that do not satisfy all of the constraints. The penalty function can be calculated as follows:

$$f_{penalty}(X) = (1 + \varepsilon_1 \cdot v)^{\varepsilon_2} . v = \sum_{i=1}^{q} v_i \tag{3}$$

where *q* is the number of frequency constraints. The values of v_i are set to zero for satisfied frequency constraints, while for violated constraints they are selected considering the severity of the violation and is defined as follows:

$$v_i = \begin{cases} 0 & if\ the\ ith\ constraint\ is\ satisfied \\ \left|1 - \frac{\omega_i}{\omega_i^*}\right| & else \end{cases} \tag{3}$$

The values for parameters ε_1 and ε_2 affect the degree to which a violated solution is penalized. They should be controlled in a way that the same amount of constraint violation results in bigger penalty values as the iterations proceeds. As a result of such a parameter selection, in the early stages, the search space is explored more freely, but in the end, they tend to choose the solutions without violation. In this study, ε_1 =1.05 and $\varepsilon_2 = 1$ for three examples.

3. METAHEURISTIC OPTIMIZATION ALGORITHM

An enhanced vibrating particle system is used to solve optimization problems in this study. The higher speed of convergence and more efficiency than VPS is the main reason to choose this algorithm for optimization. The performance process of this algorithm is expressed as follows:

First, the permissible range of initial population created by Eq. (4)

$$x_i^j = x_{min} + rand.(x_{max} - x_{min}) \tag{4}$$

where x_i^j is the *j*th variable of the *i*th particle; x_{max} and x_{min} are the upper and lower bounds of design variables in the search space, respectively.

There is another parameter called memory which saves the number of memory sizes from the best positions achieved for the population. The effect of damping level in vibration is defined according to Eq. (5)

$$D = \left(\frac{iter}{iter_{max}}\right)^{-\alpha} \tag{5}$$

where *iter* is the current number of iterations; $iter_{max}$ is the total number of iterations and α is a parameter with a constant value; ±1 is used randomly.

Finally, the new positions of the population are updated by Eq. (6)

$$x_i^j = \begin{cases} \left[D.A.rand1 + OHB^j\right] & (a) \\ \left[D.A.rand2 + GP^j\right] & (b) \\ \left[D.A.rand3 + BP^j\right] & (c) \end{cases} \tag{6}$$

Where *OHB*, *GP*, and *BP* are determined independently for each of the variables, and A is defined as follows:

$$A = \begin{cases} (\pm 1)\left(OHB^j - x_i^j\right) & (a) \\ (\pm 1)\left(GP^j - x_i^j\right) & (b) \\ (\pm 1)\left(BP^j - x_i^j\right) & (c) \end{cases} \qquad \omega_1 + \omega_2 + \omega_3 = 1 \tag{7}$$

The coefficients $\omega 1$, $\omega 2$, and $\omega 3$ are the relative importance for *OHB*, *GP*, and *BP*, respectively; *rand*1, *rand*2, and *rand*3 are random numbers uniformly distributed in the [0, 1] range.

4. NUMERICAL EXAMPLES

Three numerical examples of large-scale dome truss structures are investigated in this section for optimal design with frequency restriction using the EVPS algorithm. Some independent runs are done for each example in the optimization process. These examples include a 600-bar single-layer dome truss, an 1180-bar dome truss, and a 1410-bar double-layer dome truss. For each example, the modulus of elasticity is defined as $2 \cdot 1 \times 10^{11}$ (N/m2). The material density is 7850 $\mathrm{kg/m^3}$ for all members. A nonstructural mass of 100 kg is attached to all free nodes. the boundary of the cross-section of elements area is between $1 \times 10^{-4}\ \mathrm{m^2}$ and $1 \times 10^{-3}\ \mathrm{m^2}$. The objective function is defined as penalized weight.

4.1 600-bar dome truss

The first example is the 600-bar dome truss which is single-layer. This type of truss has been investigated by some researchers [39-41]. The structure has 216 nodes and 600 elements as

depicted in three types of view in Fig. 1. The Cartesian nodes' coordinates are presented in Table 1. The design variables are the cross-sectional area of each element, and the substructure illustrates 9 nodes and 25 elements. The optimization for this problem involves 25 design variables (cross-section groups). The angle between the two neighbor substructures is 15◦. The natural frequency constraints for this truss are defined as follows:

$$\begin{cases} \omega_1 \geq 5Hz \\ \omega_3 \geq 7Hz \end{cases} \tag{8}$$

For this example, the population size is set to 50, and the maximum number of structural analyses for is equal to 1000. The experiment is repeated 20 times, and the obtained results are presented in Table 2. The enhanced version of the VPS showed better performance in terms of best and average weight, and it converged rapidly According to the convergence curve displayed in Fig. 2.

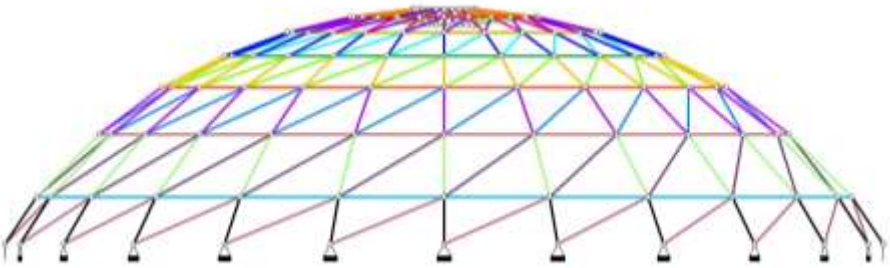

(a) Side view of 600-bar dome truss

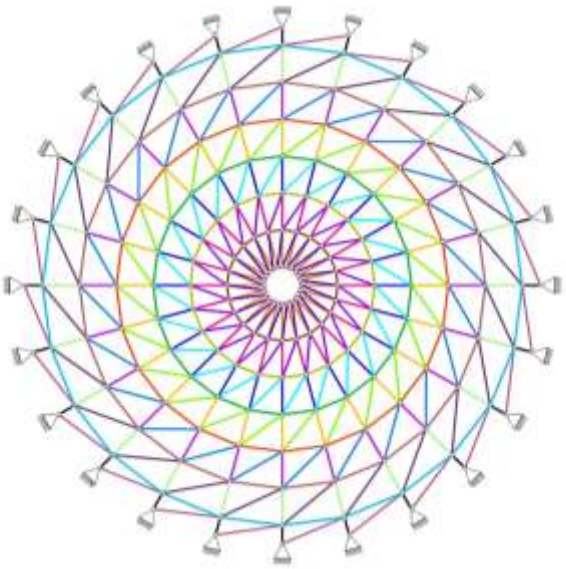

(b) Top view of 600-bar dome truss

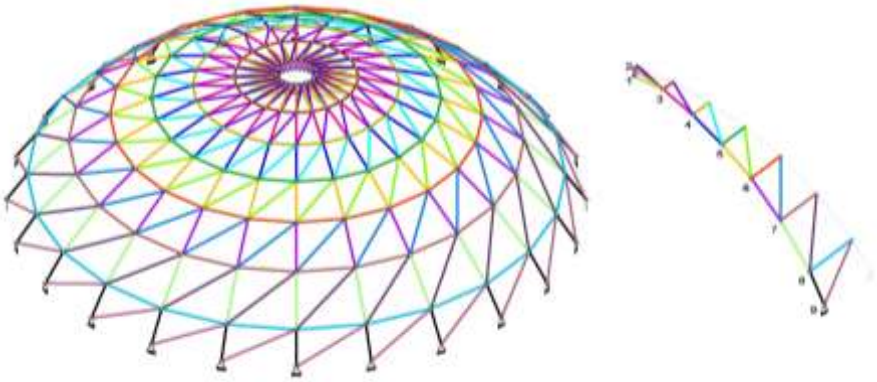

(c) Isometric view of 600-bar dome truss

Figure 1: Schematic of the 600-bar dome truss: (a) Side view, (b) Top view, (c) Isometric view

Table 1: Nodes coordinates of 600 bar dome truss

Node No.	(x,y,z)	Node No.	(x,y,z)
1	(1.0,0.0,7.0)	**6**	(9.0,0.0,5.0)
2	(1.0,0.0,7.5)	**7**	(11.0,0.0,3.5)
3	(3.0,0.0,7.25)	**8**	(13.0,0.0,1.5)
4	(5.0,0.0,6.75)	**9**	(14.0,0.0,0.0)
5	(7.0,0.0,6.0)		

Table 2: Comparison of the optimization results for 600-bar dome truss

	Cross-sectional area (cm2)				
Element No. (nodes)	**DPSO [34]**	**CBO [35]**	**ECBO [35]**	**VPS [38]**	**EVPS**
1 (1–2)	1.365	1.2404	1.4305	1.3155	1.2019
2 (1–3)	1.391	1.3797	1.3941	1.2299	1.5012
3 (1–10)	5.686	5.2597	5.5293	5.5506	5.3603
4 (1–11)	1.511	1.2658	1.0469	1.3867	1.2323
5 (2–3)	17.711	17.2255	16.9642	17.4275	16.8524
6 (2–11)	36.266	38.2991	35.1892	40.143	35.8790
7 (3–4)	13.263	12.2234	12.2171	12.8848	12.9692
8 (3–11)	16.919	15.4712	16.7152	15.5413	15.7990
9 (3–12)	13.333	11.1577	12.5999	12.2428	10.7142
10 (4–5)	9.534	9.4636	9.5118	9.3776	9.0974
11 (4–12)	9.884	8.825	8.9977	8.6684	8.0810
12 (4–13)	9.547	9.1021	9.4397	9.1659	9.2280
13 (5–6)	7.866	6.8417	6.8864	7.1664	7.4727
14 (5–13)	5.529	5.2882	4.2057	5.217	5.4983
15 (5–14)	7.007	6.7702	7.2651	6.5346	6.4660

16 (6–7)	5.462	5.1402	6.1693	5.4741	5.0321
17 (6–14)	3.853	5.1827	3.9768	3.6545	3.5817
18 (6–15)	7.432	7.4781	8.3127	7.6034	7.7686
19 (7–8)	4.261	4.5646	4.1451	4.2251	4.6190
20 (7–15)	2.253	1.8617	2.4042	1.9717	2.2625
21 (7–16)	4.337	4.8797	4.3038	4.5107	4.4862
22 (8–9)	4.028	3.5065	3.2539	3.5251	3.4169
23 (8–16)	1.954	2.4546	1.8273	1.9255	1.7917
24 (8–17)	4.709	4.9128	4.8805	4.7628	4.7613
25 (9–17)	1.41	1.2324	1.5276	1.6854	1.6376
Best weight (kg)	6344.55	6182.01	6171.51	6120.01	6067.74
Average optimized weight (kg)	6674.71	6226.37	6191.5	6158.11	6069.69
Standard deviation (kg)	473.21	60.12	39.08	28.49	3.02

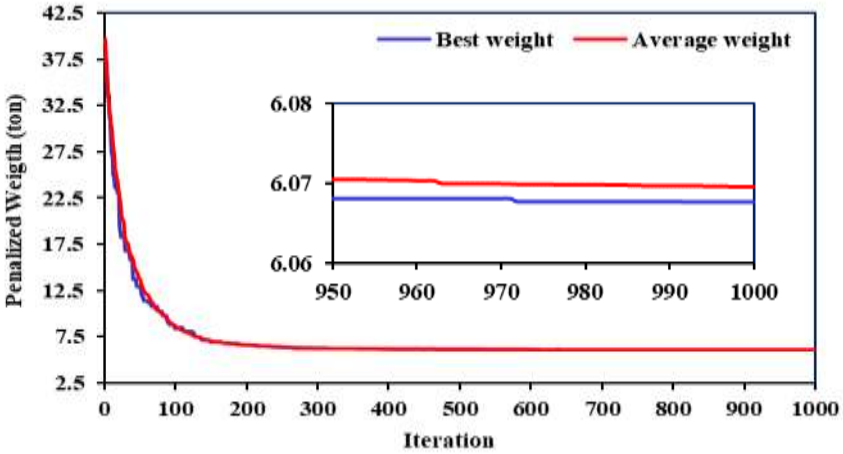

Figure 2. Convergence curve of 600-bar dome truss

4.2 1180-bar dome truss

The first example is the 1180-bar dome truss which is single-layer. This type of truss has been investigated by some researchers [42-44]. The structure has 400 nodes and 1180 elements as depicted in three types of view in Fig. 3. The Cartesian nodes' coordinates are presented in Table 3. The design variables are the cross-sectional area of each element, and the substructure illustrates 20 nodes and 59 elements. The optimization for this problem involves 59 design variables (cross-section groups). The angle between the two neighbor substructures is 18◦. The natural frequency constraints for this truss are defined as follows:

$$\begin{cases} \omega_1 \geq 7Hz \\ \omega_3 \geq 9Hz \end{cases} \quad (9)$$

For this example, the population size is set to 70, and the maximum number of structural analyses for is equal to 1000. The experiment is repeated 20 times, and the obtained results

are presented in Table 4. The enhanced version of the VPS showed better performance in terms of best and average weight, and it converged rapidly According to the convergence curve displayed in Fig. 4.

Table 3: Nodes coordinates of 1180 bar dome truss

Node No.	(x,y,z)	Node No.	(x,y,z)
1	(3.1181, 0.0, 14.6723)	**11**	(4.5788, 0.7252, 14.2657)
2	(6.1013, 0.0, 13.7031)	**12**	(7.4077, 1.1733, 12.9904)
3	(8.8166, 0.0, 12.1354)	**13**	(9.9130, 1.5701, 11.1476)
4	(11.1476, 0.0, 10.0365)	**14**	(11.9860, 1.8984, 8.8165)
5	(12.9904, 0.0, 7.5000)	**15**	(13.5344, 2.1436, 6.1013)
6	(14.2657, 0.0, 4.6358)	**16**	(14.4917, 2.2953, 3.1180)
7	(14.9179, 0.0, 1.5676)	**17**	(14.8153, 2.3465, 0.0)
8	(14.9179, 0.0, - 1.5677)	**18**	(14.4917, 2.2953, - 3.1181)
9	(14.2656, 0.0, - 4.6359)	**19**	(13.5343, 2.1436, - 6.1014)
10	(12.9903, 0.0, - 7.5001)	**20**	(3.1181, 0.0, 13.7031)

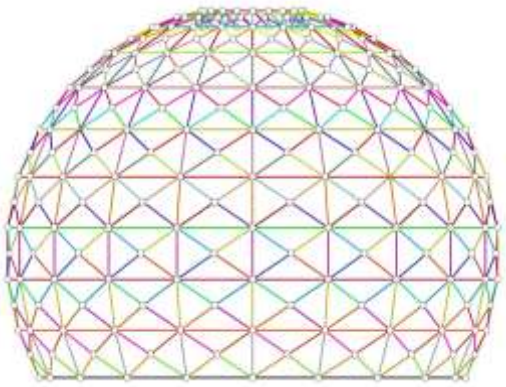

(a) Side view of 1180-bar dome truss

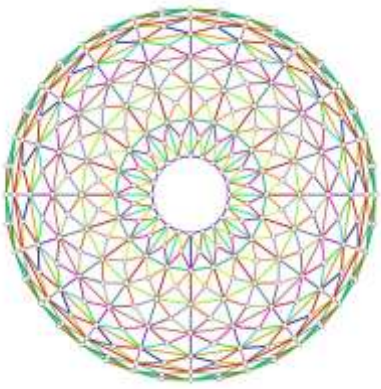

Top view of 1180-bar dome truss

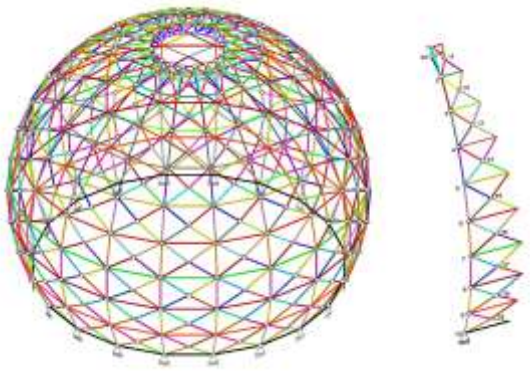

(C) Isometric view of 1180-bar dome truss

Figure 3: Schematic of the 1180-bar dome truss: (a) Side view, (b) Top view, (c) Isometric view

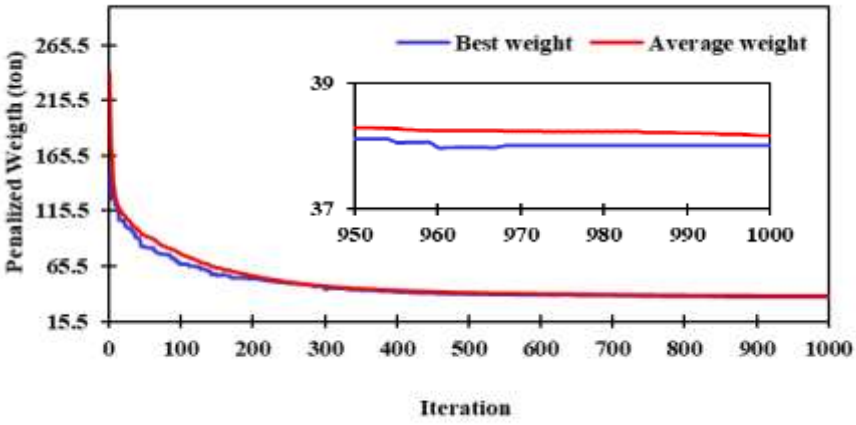

Figure 4: Convergence curve of 1180-bar dome truss

Table 4: Comparison of the optimization results for 1180-bar dome truss

	Cross-sectional area (cm2)				
Element No. (nodes)	**DPSO [34]**	**CBO [35]**	**ECBO [37]**	**VPS [38]**	**EVPS**
1 (1–2)	7.926	13.0171	7.6678	6.8743	8.2704
2 (1–11)	10.426	10.4346	11.1437	10.023	9.0477
3 (1–20)	2.115	3.0726	1.852	4.414	2.4083
4 (1–21)	14.287	12.6969	14.5563	13.5515	17.6548
5 (1–40)	3.846	3.5654	4.9499	1.8303	5.0107
6 (2–3)	5.921	6.519	6.8095	7.0824	6.8212
7 (2–11)	7.955	7.4233	6.6803	6.396	5.5067
8 (2–12)	6.697	6.3471	6.7889	6.5646	6.3639
9 (2–20)	1.889	2.3013	1.063	2.3705	2.3437

10 (2–22)	11.881	12.1936	9.1602	13.2621	11.4931
11 (3–4)	7.121	7.2877	6.9891	7.0922	7.6098
12 (3–12)	6.080	7.0961	6.9881	6.8079	6.0982
13 (3–13)	6.599	6.5669	6.9555	6.3815	6.5201
14 (3–23)	7.772	7.8257	7.5443	7.3122	7.6463
15 (4–5)	9.358	8.6812	9.5431	8.7221	10.5859
16 (4–13)	6.213	5.7888	6.9123	6.368	6.3780
17 (4–14)	8.200	21.1342	8.9891	7.3159	7.0271
18 (4–24)	7.799	10.0502	6.8926	11.5749	7.9658
19 (5–6)	11.752	12.9279	12.6128	14.7985	12.0607
20 (5–14)	7.494	9.3212	8.1983	5.5174	8.3980
21 (5–15)	9.696	10.126	11.8358	15.7381	12.5623
22 (5–25)	9.177	10.1358	9.7321	8.3419	9.2832
23 (6–7)	17.326	15.8585	19.165	17.5	17.0449
24 (6–15)	11.797	9.9672	10.4682	10.3084	11.0122
25 (6–16)	14.002	14.8493	14.1178	15.1958	14.7680
26 (6–26)	11.562	11.4909	11.14567	10.9395	10.9959
27 (7–8)	23.981	26.2359	23.4125	24.9421	21.9150
28 (7–16)	12.996	13.8812	15.5167	13.9614	16.1827
29 (7–17)	16.591	18.8857	16.6613	18.4153	20.8216
30 (7–27)	15.910	14.0257	15.9631	14.4945	18.0993
31 (8–9)	34.642	33.8826	37.0532	36.3529	34.2502
32 (8–17)	19.860	25.7142	22.2937	19.6608	16.8668
33 (8–18)	25.079	24.8644	22.7409	23.7259	25.6881
34 (8–28)	18.965	19.8498	23.5624	22.0297	22.3720
35 (9–10)	47.514	53.263	47.7652	47.3286	46.6206
36 (9–18)	28.133	22.7771	22.5066	22.9442	22.0552
37 (9–19)	33.023	35.423	34.6418	30.8229	28.4370
38 (9–29)	32.263	57.548	31.6492	33.1098	29.5337
39 (10–19)	33.401	35.1385	32.7268	32.5526	36.8086
40 (10–30)	1.344	10.73	1.05206	1.7363	1.5819
41 (11–21)	9.327	9.2401	11.3681	11.5271	8.7834
42 (11–22)	7.202	5.2661	6.5512	8.4571	6.3483
43 (12–22)	6.792	6.2415	6.3619	5.4136	5.6296
44 (12–23)	6.228	4.4768	5.9296	7.1832	5.6345
45 (13–23)	6.601	8.8846	7.8739	5.4066	6.4783
46 (13–24)	6.584	7.371	6.2794	6.2534	6.3008
47 (14–24)	8.320	8.2595	7.6206	6.9383	8.7835
48 (14–25)	8.844	7.6091	7.2937	10.6872	7.3685
49 (15–25)	11.254	11.303	10.5783	12.8005	11.9231
50 (15–26)	12.162	13.8381	10.1173	10.2216	10.1779
51 (16–26)	13.854	13.3654	15.1088	11.533	13.9712
52 (16–27)	13.844	13.1836	12.8251	11.6918	13.1250
53 (17–27)	17.536	13.5793	17.4375	20.7566	17.0503

54 (17–28)	20.551	10.0628	20.1153	18.1341	23.0291
55 (18–28)	24.072	24.1197	24.2121	28.2882	23.4632
56 (18–29)	27.287	24.2604	23.3175	24.2023	23.4265
57 (19–29)	32.965	34.1389	34.6196	48.018	35.9923
58 (19–30)	36.940	38.034	35.297	35.6517	42.7071
59 (20–40)	3.837	2.6689	8.8569	5.5956	5.0568
Best weight (kg)	37779.81	40,985	37984.39	38699.14	38008.9
Average optimized weight (kg)	38294.45	42019.10	38042.15	38861.82	38171.95
Standard deviation (kg)	550.5	655.72	101.43	385.41	139.41

4.3 1410-bar dome truss

The first example is the 1410-bar dome truss which is double-layer. This type of truss has been investigated by some researchers [45-47]. The structure has 390 nodes and 1410 elements as depicted in three types of view in Fig. 5. The Cartesian nodes' coordinates are presented in Table 5. The design variables are thecross-sectional area of each element, and the substructure illustrates 13 nodes and 47 elements. The optimization for this problem involves 47 design variables (cross-section groups). The angle between the two neighbor substructures is 12◦. The natural frequency constraints for this truss are defined as follows:

$$\begin{cases} \omega_1 \geq 7Hz \\ \omega_3 \geq 9Hz \end{cases} \quad (10)$$

For this example, the population size is set to 55, and the maximum number of structural analyses for is equal to 1000. The experiment is repeated 20 times, and the obtained results are presented in Table 6. The enhanced version of the VPS showed better performance in terms of best and average weight, and it converged rapidly According to the convergence curve displayed in Fig. 6.

Table 5: Nodes coordinates of 1410 bar dome truss

Node No.	(x,y,z)	Node No.	(x,y,z)
1	(1.0, 0.0, 4.0)	**8**	(1.989, 0.209, 3.0)
2	(3.0, 0.0, 3.75)	**9**	(3.978, 0.418, 2.75)
3	(5.0, 0.0, 3.25)	**10**	(5.967, 0.627, 2.25)
4	(7.0, 0.0, 2.75)	**11**	(7.956, 0.836, 1.75)
5	(9.0, 0.0, 2.0)	**12**	(9.945, 1.0453, 1.0)
6	(11.0, 0.0, 1.25)	**13**	(11.934, 1.2543, - 0.5)
7	(13.0, 0.0, 0.0)		

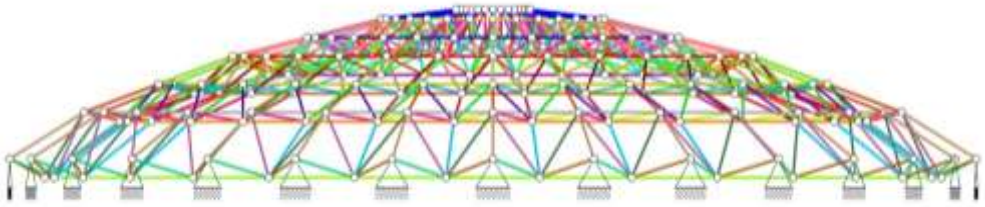

(a) Side view of 1410-bar dome truss

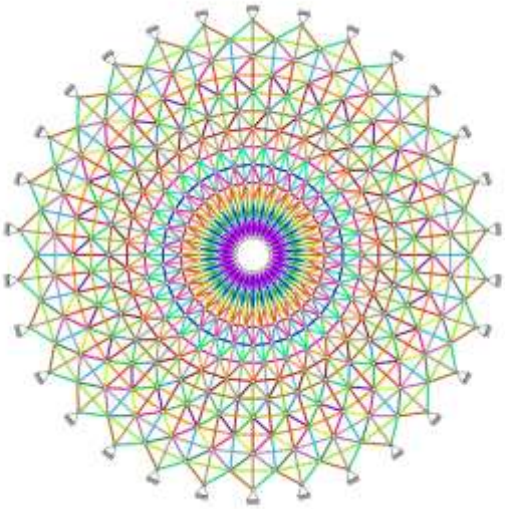

(b) Top view of 1410-bar dome truss

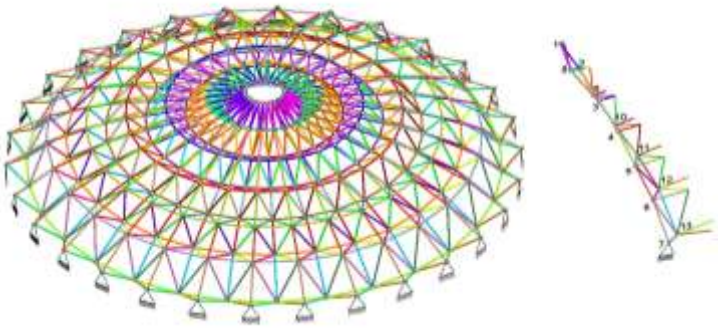

(c) Isometric view of 1410-bar dome truss

Figure 5: Schematic of the 1410-bar dome truss: (a) Side view, (b) Top view, (c) Isometric view

Table 6: Comparison of the optimization results for 1410-bar dome truss

	Cross-sectional area (cm2)				
Element No. (nodes)	**DPSO [34]**	**CBO [35]**	**ECBO [37]**	**VPS [38]**	**EVPS**
1 (1–2)	7.209	1.0073	7.7765	5.6333	6.9338
2 (1–8)	5.006	2.5808	6.2173	4.7628	4.7701
3 (1–14)	38.446	24.3407	23.9162	37.7385	29.4676
4 (2–3)	9.438	6.675	11.2399	7.4927	10.3698
5 (2–8)	4.313	3.8881	2.5775	3.1824	5.8838
6 (2–9)	1.494	5.0607	1.8559	1.0193	2.0475
7 (2–15)	8.455	78.9781	16.9202	8.9475	15.0685
8 (3–4)	9.488	9.2944	13.7947	10.4272	9.1870
9 (3–9)	3.480	2.6585	5.4502	4.1398	2.5231
10 (3–10)	3.495	3.5399	2.9751	3.1408	3.1458
11 (3–16)	16.037	10.2473	13.7811	15.4194	8.5578
12 (4–5)	9.796	9.682	9.387	8.9931	9.0714
13 (4–10)	2.413	2.4435	2.3499	3.1988	2.0449
14 (4–11)	5.681	5.0637	4.9125	7.1565	4.4520
15 (4–17)	15.806	12.9434	11.8755	17.8564	15.5304
16 (5–6)	8.078	6.9073	8.8668	9.2685	8.0463
17 (5–11)	3.931	3.1808	3.6304	3.3221	4.1273
18 (5–12)	6.099	5.9622	6.2651	6.1486	5.8742
19 (5–18)	10.771	13.3195	15.103	8.4422	12.2753
20 (6–7)	13.775	13.2136	13.1091	12.8578	13.8096
21 (6–12)	4.231	5.4405	5.294	5.8031	5.5497
22 (6–13)	6.995	8.4703	5.9929	7.5484	7.8487
23 (6–19)	1.837	1.87	1	1.4805	1.2083
24 (7–13)	4.397	5.5203	4.9879	4.5332	4.4281
25 (8–9)	2.115	2.4492	3.178	2.0347	3.4544
26 (8–14)	4.923	2.215	5.9226	5.8589	4.7012
27 (8–15)	4.047	3.1193	2.4607	2.4401	6.5027
28 (8–21)	5.906	8.7508	7.571	6.925	14.0563
29 (9–10)	3.392	5.1195	4.8616	3.3875	3.7540
30 (9–15)	1.902	3.8508	1.5956	1.5024	1.8509
31 (9–16)	4.381	4.4435	4.9084	4.0498	3.6430
32 (9–22)	8.442	9.1339	11.6118	11.0886	4.6275
33 (10–11)	5.011	5.7811	5.2554	5.4639	6.1824
34 (10–16)	3.577	3.451	2.8687	2.8459	2.6757
35 (10–17)	2.805	1.8344	2.3286	2.3136	2.2184
36 (10–23)	2.024	2.7952	1.6159	3.437	1.2067
37 (11–12)	6.709	7.2668	6.9795	8.0225	6.8483
38 (11–17)	5.054	4.7761	5.3159	5.8009	4.0047
39 (11–18)	3.259	3.3394	2.9915	4.4004	3.8577
40 (11–24)	1.063	1.0001	1.0018	1.0005	1.2502
41 (12–13)	5.934	7.3874	4.1091	7.7222	5.7831
42 (12–18)	7.057	7.3114	6.013	5.2574	5.6696

43 (12–19)	5.745	4.8773	5.8695	4.5055	6.2424
44 (12–25)	1.185	1	1	1.0005	1.6216
45 (13–19)	7.274	7.9928	7.7041	7.9383	6.6286
46 (13–20)	4.798	3.4989	3.76	4.7805	4.6648
47 (13–26)	1.515	2.0951	1.0006	1.0054	1.0336
Best weight (kg)	10453.84	11102.84	10739.19	10491.83	10391.51
Average optimized weight (kg)	11100.57	12359.41	10812.20	10936.34	10412.82
Standard deviation (kg)	334.2	251.88	64.91	158.39	41.10

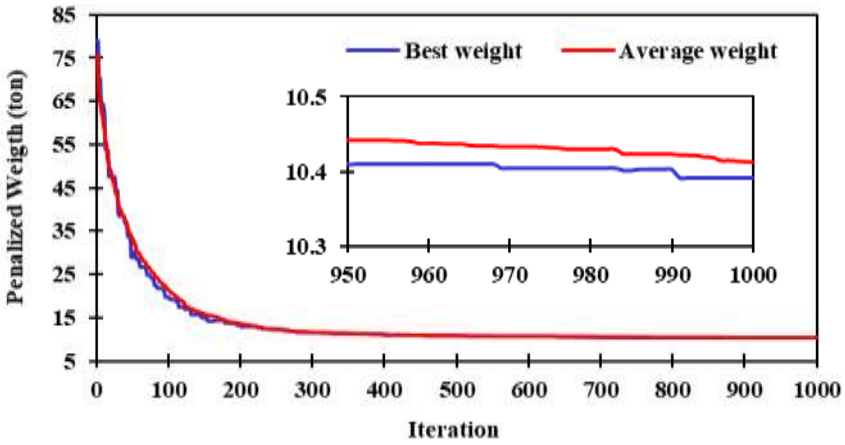

Figure 6. Convergence curve of 1410-bar dome truss

The results of frequency limitations for each dome trusses are presented in Table 8.

Table 8: Frequency constraints of three large-scale dome trusses

Structures	Frequency limitation value	EVPS
600-bar	$\omega_1 = 5$	5.0005
	$\omega_2 = 7$	7.0002
1180-bar	$\omega_1 = 7$	7.0003
	$\omega_2 = 9$	9.012
1410-bar	$\omega_1 = 7$	7.003
	$\omega_2 = 9$	9.001

5. CONCLUSION

Optimum design of the structure with natural frequency limitations is a challenging class of optimization problems characterized by highly nonlinear and non-convex search spaces with numerous local optima. Structural optimization using meta-heuristic methods needs thousands of structural analyses. These analyses require a great deal of computational time,

especially when the structures are large scale. This paper investigates an enhanced vibrating particles system to find the optimum design for this kind of problem. Since this algorithm has performed successfully in previous studies, three numerical examples are investigated to prove the efficiency of the proposed method in solving the optimization problem. The results indicate that the proposed algorithm can obtain an acceptable solution, and is able of finding lighter structures compared to DPSO, CBO, ECBO, and VPS, which are all among powerful meta-heuristic algorithms.

REFERENCES

1. Grandhi R. Structural optimization with frequency constraints—a review, *AIAA J* 1993; **31**: 2296-303.
2. Das S, Saha P. Performance of swarm intelligence based chaotic meta-heuristic algorithms in civil structural health monitoring, *Measure* 2021; **169**(108529).
3. Housseina E, Saad MR, Hashim FA, Shaban H, Hassaballah M. Lévy flight distribution: A new metaheuristic algorithm for solving engineering optimization problems, *Eng Applicat Artificial Intell* 2020; **94**(103731).
4. Ficarella E, Lamberti L, Degertekin FO. Comparison of three novel hybrid metaheuristic algorithms for structural optimization problems, *Comput Struct* 2021; **244**(106395).
5. Kaveh A, Zolghadr A. Democratic PSO for truss layout and size optimization with frequency constraints, *Comput Struct* 2014; **130**: 10-21.
6. Kaveh A, Mahdavi VR. Colliding-bodies optimization for truss optimization with multiple frequency constraints, *Adv Eng Softw* 2014; **70**: 1-12.
7. Kaveh A, Ilchi Ghazaan M. Enhanced colliding bodies optimization for design problems with continuous and discrete variables, *Adv Eng Softw* 2014; **77**: 66-75.
8. Kaveh A, Farhoudi N. A new optimization method: Dolphin echolocation, *Adv Eng Softw* 2013; **59**: 53–70.
9. Jalil Sh, Hosseinzadeh Y. Combining migration and differential evolution strategies for optimum design of truss structures with dynamic constraints, *Iranian J Sci Technol, Transact Civil Eng* 2018; **43**: 289–312.
10. Kaveh A, Biabani Hamedani K, Kamalinejad M, Joudaki A. Quantum-Based jellyfish search optimizer for structural optimization, *Int J Optim Civil Eng* 2021; **11**(2): 329-56.
11. Millan-Paramo C, Filho JEA. Size and shape optimization of truss structures with natural frequency constraints using modified simulated annealing algorithm, *Arabian J Sci Eng* 2020; **45**: 3511-25.
12. Jalili Sh, Hosseinzadeh Y, Rabczuk T. Simultaneous size and shape optimization of dome-shaped structures using improved cultural algorithm, *Socio-Cultu Inspir Metaheur* 2019; 93-119.
13. Grzywiński M, Selejdak J, Dede T. Truss optimization with frequency constraints based on TLBO algorithm, *AIP Conference Proceedings* 2020; 2239.
14. Millán-Páramo C, Millán-Romero E, Wilches FJ. Truss optimization with natural frequency constraints using modified social engineering optimizer, *Int J Eng Res Technol* 2020; **13**(11): 3950-63.
15. Jalil Sh, Talatahari S. Optimum design of truss structures under frequency constraints using hybrid CSS-MBLS algorithm, *KSCE J Civil Eng* 2018; **22**(5): 1840-53.

16. Kaveh A, Biabani K, Kamalinejad M. An enhanced forensic-based investigation algorithm and its application to optimal design of frequency-constrained dome structures, *Comput Struct* 2021; **256**.
17. Tejani G, Savani J, Patel VK, Mirjalili SA. Truss optimization with natural frequency bounds using improved symbiotic organisms search, *Knowle-Based Syst* 2017; 1-17.
18. Makiabadi M, Maheri MR. An enhanced symbiotic organisms search algorithm for design optimization of trusses with frequency constraints, *Adv Struct Eng* 2021; **24**(14): 3315-37.
19. Lemonge ACC, Carvalho JPG, Hallak PH, Vargas DEC. Multi-objective truss structural optimization considering natural frequencies of vibration and global stability, *Expert Syst Applicat* 2021; **165:** 113777.
20. Liu S, Zho H, Chen Z, Cao H. Frequency-constrained truss optimization using the fruit fly optimization algorithm with an adaptive vision search strategy, *Eng Optim* 2020; **52**(5): 777-97.
21. Kaveh A, Zolghadr A. Optimal design of cyclically symmetric trusses with frequency constraints using cyclical parthenogenesis algorithm, *Adv Struct Eng* 2018; **21**(5).
22. Shahrouzi M, Rafiee F, Aghabaglou M. Configuration design of structures under dynamic constraints by a hybrid bat algorithm and teaching–learning based optimization, *Int J Dyn Control* 2019; **7**: 419-29.
23. Kaveh A, Amirsoleimani P, Dadras Eslamlou A, Rahmani P. Frequency-constrained optimization of large-scale dome-shaped trusses using chaotic water strider algorithm, *Struct* 2021; **32**: 1604-18.
24. Kaveh A, Javadi SM. Chaos-based firefly algorithms for optimization of cyclically large-size braced steel domes with multiple frequency constraints, *Comput Struct* 2019; **214**: 28-39.
25. Kaveh A, Malakouti Rad S. Hybrid genetic algorithm and particle swarm optimization for the force method-based simultaneous analysis and design, *Iranian J Sci Technol* 2010; **34** (1): 15-34.
26. Kaveh A, Talatahari S. Hybrid charged system search and particle swarm optimization for engineering design problems, *Eng Computat* 2011; **28**(4): 423-40.
27. Kaveh A, M. Ilchi Ghazaan. A new meta-heuristic algorithm: Vibrating particles system, *Sci Iran* 2017; **24**(2): 551-66.
28. Kaveh A, M. Khosravian. Size/layout optimization of truss structures using vibrating particles system meta-heuristic algorithm and its improved version, *Period Polytech Civil Eng* 2022; **66**(1): 1–17.
29. Kaveh A, Hoseini Vaez SR, Hosseini P. Matlab code for an enhanced vibrating particles system algorithm, *Int J Optim Civil Eng* 2018; **8**(3): 104-14.
30. Kaveh A, Hoseini Vaez SR, Hosseini P. Enhanced vibrating particles system algorithm for damage identication of truss structures, *Sci Iran* 2019; **26**(1): 246-56.
31. Kaveh A, Hoseini Vaez SR, Hosseini P. Performance of the modified dolphin monitoring operator for weight optimization of skeletal structures, *Period Polytech Civil Eng* 2019; **63**(1): 30-45.
32. Kaveh A, Hoseini Vaez SR, Hosseini P, Abedini H. Weight minimization and energy dissipation maximization of braced frames using EVPS algorithm, *Int J Optim Civil Eng* 2020; **10**(3): 513-29

33. Hosseini P, Hoseini Vaez SR, Fathali MA, Mehanpour H. Reliability assesment of transmission line towers using metaheuristic algorithms, *Int J Optim Civil Eng* 2020; **10**(3): 531-51
34. Kaveh A, Hoseini Vaez SR, Hosseini P, Fathi H. Crack detection with XFEM in plate structures using MDM operator, *Int J Optim Civil Eng* 2021; **11**(2): 231-48
35. Kaveh A, Hoseini Vaez SR, Hosseini P, Fathali MA. Heuristic operator for reliability assessment of frame structures, *Period Polytech Civil Eng* 2021; **65**(3): 702-16.
36. Kaveh A, Zolghadr A. Optimal analysis and design of large-scale domes with frequency constraints. *Applicat Metaheuris Optim Algorith Civil Eng* 2016; 257-79.
37. Kaveh A, Ilchi Ghazaan M. editors. *Meta-heuristic Algorithms for Optimal Design of Real-Size Structures*, Cham: Springer International Publishing, 2018.
38. Kaveh A, Ilchi Ghazaan M. A new hybrid meta-heuristic algorithm for optimal design of large-scale dome structures, *Eng Optim* 2018; **50**(2).
39. Kaveh A, Ilchi Ghazaan M, Saadatmand F. Colliding bodies optimization with Morlet wavelet mutation and quadratic interpolation for global optimization problems, *Eng Comput* 2021.
40. Kaveh A, Biabani K, Kamalinejad M. Improved arithmetic optimization algorithm for dtructural optimization with frequency constraints, *Int J Optim Civil Eng* 2021; **11**(4): 663-93.
41. Kaveh A, Biabani K, Joudaki A, Kamalinejad M. Optimal analysis for optimal design of cyclic symmetric structures subject to frequency constraints, *Struct* 2021; **33**: 3122-36.
42. Dede T, Grzywinski M, Selejdak J. Continuous size optimization of large-scale dome structures with dynamic constraints, *Struct Eng Mech* 2020; **73**(4): 397-405.
43. Kaveh A, Ghazaan M. Optimal design of dome truss structures with dynamic frequency constraints, *Struct Multidisc Optim* 2016; **53**: 605–21.
44. Kaveh A, Zolghadr A. Meta-heuristic methods for optimization of truss structures with vibration frequency constraints, *Acta Mech* 2018; **229**: 3971-92.
45. José PG, Carvalho EA. Truss optimization with multiple frequency constraints and automatic member grouping, *Struct Multidisc Optim* 2018; **57**: 547-77.
46. José PG. Carvalho EA. Simultaneous sizing, shape, and layout optimization and automatic member grouping of dome structures, *Struct* 2020; **28**: 2188-2202.
47. Kaveh A, Javadi SM. Chaos-based firefly algorithms for optimization of cyclically large-size braced steel domes with multiple frequency constraints, *Comput Struct* 2019; **214**: 28-39.